Reservoir operation based on evolutionary algorithms and multi-criteria decision-making under climate change and uncertainty

Mohammad Ehteram, Sayed Farhad Mousavi, Hojat Karami, Saeed Farzin, Vijay P. Singh, Kwok-wing Chau and Ahmed El-Shafie

ABSTRACT

This study investigated reservoir operation under climate change for a base period (1981–2000) and future period (2011–2030). Different climate change models, based on A2 scenario, were used and the HAD-CM3 model, considering uncertainty, among other climate change models was found to be the best model. For the Dez basin in Iran, considered as a case study, the climate change models predicted increasing temperature from 1.16 to 2.5°C and decreasing precipitation for the future period. Also, runoff volume for the basin would decrease and irrigation demand for the downstream consumption would increase for the future period. A hybrid framework (optimization-climate change) was used for reservoir operation and the bat algorithm was used for minimization of irrigation deficit. A genetic algorithm and a particle swarm algorithm were selected for comparison with the bat algorithm. The reliability, resiliency, and vulnerability indices, based on a multi-criteria model, were used to select the base method for reservoir operation. Results showed the volume of water to be released for the future period, based on all evolutionary algorithms used, was less than for the base period, and the bat algorithm with high-reliability index and low vulnerability index performed better among other evolutionary algorithms.

Key words | bat algorithm, climate change, reservoir operation, water resource management

Mohammad Ehteram
Sayed Farhad Mousavi
Hojat Karami (corresponding author)
Saeed Farzin
Department of Water Engineering and Hydraulic Structures, Faculty of Civil Engineering,
Semnan University,
Semnan, Iran
E-mail: *hkarami@semnan.ac.ir*

Vijay P. Singh
Department of Biological and Agricultural Engineering, Zachry Department of Civil Engineering,
Texas A and M University,
321 Scoates Hall, 2117 TAMU, College Station,
Texas 77843-2117, USA

Kwok-wing Chau
Department of Civil and Environmental Engineering,
Hong Kong Polytechnic University,
Hung Hom, Kowloon, Hong Kong

Ahmed El-Shafie
Department of Civil Engineering, Faculty of Engineering,
University of Malaya, Malaysia

INTRODUCTION

Water scarcity and climate change pose serious challenges for decision-makers with regard to water supply during critical and drought periods (Gohari *et al.* 2017). Increased greenhouse gases and growing population complicate resources allocation and management (Kamperman & Biesbroek 2017). Reservoir operation, runoff simulation, and water allocation are important in water resource management. Climate change is triggering temperature increase and is impacting the quality and quantity of water available in reservoirs, runoff, and sediment load (Intergovernmental Panel on Climate Change (IPCC) 2014). Industrial countries with their large gas emissions and countries with emerging economies combine to cause climate change which then is being alleged to be causing sea level rise, tropical storms, and floods and droughts. Thus, prediction of weather extremes and their impact on available resources is necessary (Beermann 2017).

Background

In recent years, mathematical models and climate change scenarios have been combined in order to achieve better

doi: 10.2166/hydro.2018.094

management of water supply (Santos *et al.* 2017). These mathematical models are used for prediction of demand, water supply, runoff, and flood control for the future and base periods. Buchtele (1993) applied different climate change scenarios and models for the prediction of runoff from a basin. Investigating the uncertainty of different climate change models, the Had-CM3 model was found to be having the lowest uncertainty and then the HEC-HMS model was used for the prediction of runoff in the base and future periods. High correlation index and low mean absolute error showed that the model was accurate and the runoff volume would decrease for the period of 2000–2020.

Burn & Simonovic (1996) investigated the change in water release under climate change and different scenarios of inflow to the reservoir. The runoff volume for the period of 2000–2020 was predicted as inflow to the reservoir and with the computed inflow or runoff the volume of water release was computed using Lingo software. The water release curve and comparison with demand values showed that the reliability index of the reservoir for water supply decreased for the future period as compared to the base period (1980–2000).

Xu (1999) used general circulation models (GCMs) for the prediction of temperature and precipitation and then these values were used for runoff prediction using hydrological models. One of the important issues was related to the large scale of computational cells in the GCMs which were introduced by different downscaling methods.

A conceptual monthly water balance model, based on 15 climate change scenarios, was used for flow prediction in the central basin in Sweden (Xu 2000), and results showed decreasing snow and flow volume for the period of 2000–2025.

In another study, an artificial neural network (ANN) was used for flow prediction under climate change. First, temperature and precipitation were computed for the period of 1980–2000 and then these values were used as inflow for runoff prediction in the future period. The ANN was found to perform well under climate change (Agarwal & Singh 2004).

Alfieri *et al.* (2006) computed the change in power production of a powerhouse for the water released from an upstream dam for the period 2000–2025 under climate change. Nonlinear programming was used for minimizing an objective function with the aim of decreasing the hydropower shortage downstream. Results showed that the power supply under climate change was in accordance with higher vulnerability index for the future periods.

Water allocation under climate change and uncertainty of climate change models were investigated in another case study (Wang *et al.* 2008). A weighting method based on a probability density function (PDF) was used for the determination of uncertainty and the selection of the best model. The Had-CM3 model was used and for temperature and precipitation values and using the predicted runoff, water allocation was then done for the future period 1990–2010.

Kisi (2011) applied a wavelet regression model (WRM) for runoff prediction under climate change for a future period. The A2 scenario and five climate change models were used for temperature and precipitation. Runoff was predicted using WRM and ANN where WRM was more accurate for runoff prediction for the base period.

The LARS-WG model was used in another study for downscaling of GCMs with high accuracy and then with predicted temperature and precipitation, irrigation water demands were predicted (Hassan *et al.* 2014).

A multi-objective problem of reservoir operation with the aim of increasing the reliability index and decreasing the vulnerability index under climate change was investigated for the prediction of water to be released from a multi-reservoir system. A hybrid framework of multi-objective genetic algorithm and climate change model was used for the computation of rule curves and the computed curves showed decreasing reliability index and increasing vulnerability index for the period 2046–2065 (Ahmadi *et al.* 2014).

Ashofteh *et al.* (2017a) applied a dynamic system (WEAP model) for water resources management in a basin in Iran for a future period (2046–2065) under climate change. Results showed the inflow to the reservoir in the basin decreased and the demand for irrigation increased compared to the base period. A dynamic model (ZRW-MSM 2.0) was used in another study to investigate the effect of climate change on water resources management of a basin in Iran. Results reported population and drought growth for the future period with the increase of demands (Gohari *et al.* 2017).

Ashofteh *et al.* (2017b) applied the logic genetic programming method for reservoir operation under climate change and found that logic genetic programming had a smaller value for the objective function, the reliability index for water supply for the future period decreased, and the vulnerability index increased for the future period compared to the base period.

Ashofteh *et al.* (2017c) applied multi-objective genetic programming for reservoir operation with the aim of increasing reliability and decreasing vulnerability. The rule curve for irrigation demand obtained from this programming showed less shortage index for the period of 2026–2039.

Applying two-dimensional dynamic programming for reservoir operation under climate change, Zhang *et al.* (2017) showed that the fixed rule curve could not respond to the demand for the future period and hence used adaptive rule curves for the future period.

Using multi-objective genetic algorithm for reservoir operation for power and water supply considering climate change, Yang *et al.* (2017b) showed that it was capable of supplying 300 million m^3/year of water for the future period.

Neural network and support vector machine were used for prediction of inflow to a reservoir under climate change by Yang *et al.* (2017a), who found that runoff decreased for the future period compared to the base period and there was uncertainty in different climate change models for runoff volume.

Previous studies have investigated water resources management under climate change. In this study, a new hybrid framework, based on an artificial intelligence method and climate change models, is used for the operation of a reservoir in Iran. First, temperature and precipitation based on climate change methods are computed for the base period (1981–2000) and the future period (2011–2030) and then the IHACERS software as a hydrological model is used for the prediction of runoff. The predicted runoff is used as inflow to the reservoir and the bat algorithm as an artificial intelligence method is used for the minimization of irrigation deficit downstream because meta-heuristic algorithms have been successfully applied to reservoir operation (Fallah-Mehdipour *et al.* 2011, 2013). For example, Wang *et al.* (2011) applied an interactive genetic algorithm for reservoir operation and results showed this method was accurate and its solution was closer to the global solution compared to a nonlinear programming method. Ostadrahimi *et al.* (2012) applied a particle swarm optimization algorithm (PSOA) for the operation of a multi-reservoir system with the aim to supply demands and the algorithm exhibited faster convergence. Asgari *et al.* (2015) used a weed algorithm for reservoir optimization with the aim to decrease irrigation shortage and the algorithm yielded solutions closer to the global solution. The bat algorithm is one the newest algorithms to be used in engineering optimization. In this study, this algorithm was used for optimization of reservoir operation.

The reason for applying the bat algorithm to reservoir operation is its high potential for optimization. Niknam *et al.* (2013) applied this algorithm with the aim to increase energy production. Results showed that the algorithm converges in less time than did the genetic algorithm and particle swarm algorithm. Bozorg-Haddad *et al.* (2014) used the bat algorithm for reservoir operation with the aim to decrease hydropower shortage and results showed that the algorithm had a higher ability to find the global solution than the other evolutionary algorithms or traditional methods, such as nonlinear programming method or dynamic programming method.

Problem statement, innovation, and objective

When demand and water resources are to be predicted for future periods, the methods with higher reliability should be employed. The hydrological method and artificial intelligence methods can be combined as a hybrid framework for water resources management. The difference between the current study and previous studies is the combination of climate change with the bat algorithm for reservoir operation optimization and hydrological model, while the previous studies, such as Bozorg-Haddad *et al.* (2014) and Ahmadianfar *et al.* (2015) investigated reservoir operation based on the bat algorithm without the consideration of climate change and its effect on reservoir operation. In this study, one can use the hybrid framework for other reservoir operation problems. Figure 1 shows the flowchart of the model procedure including the major stages at different levels of this study. In addition, the other key point is the computation of uncertainty of climate change models based on the Bayesian statistical method which determines the more reliable climate model for the next application, such as runoff simulation. Furthermore, the genetic algorithm and the particle swarm algorithm were used for comparison with the bat algorithm and a multi-criteria

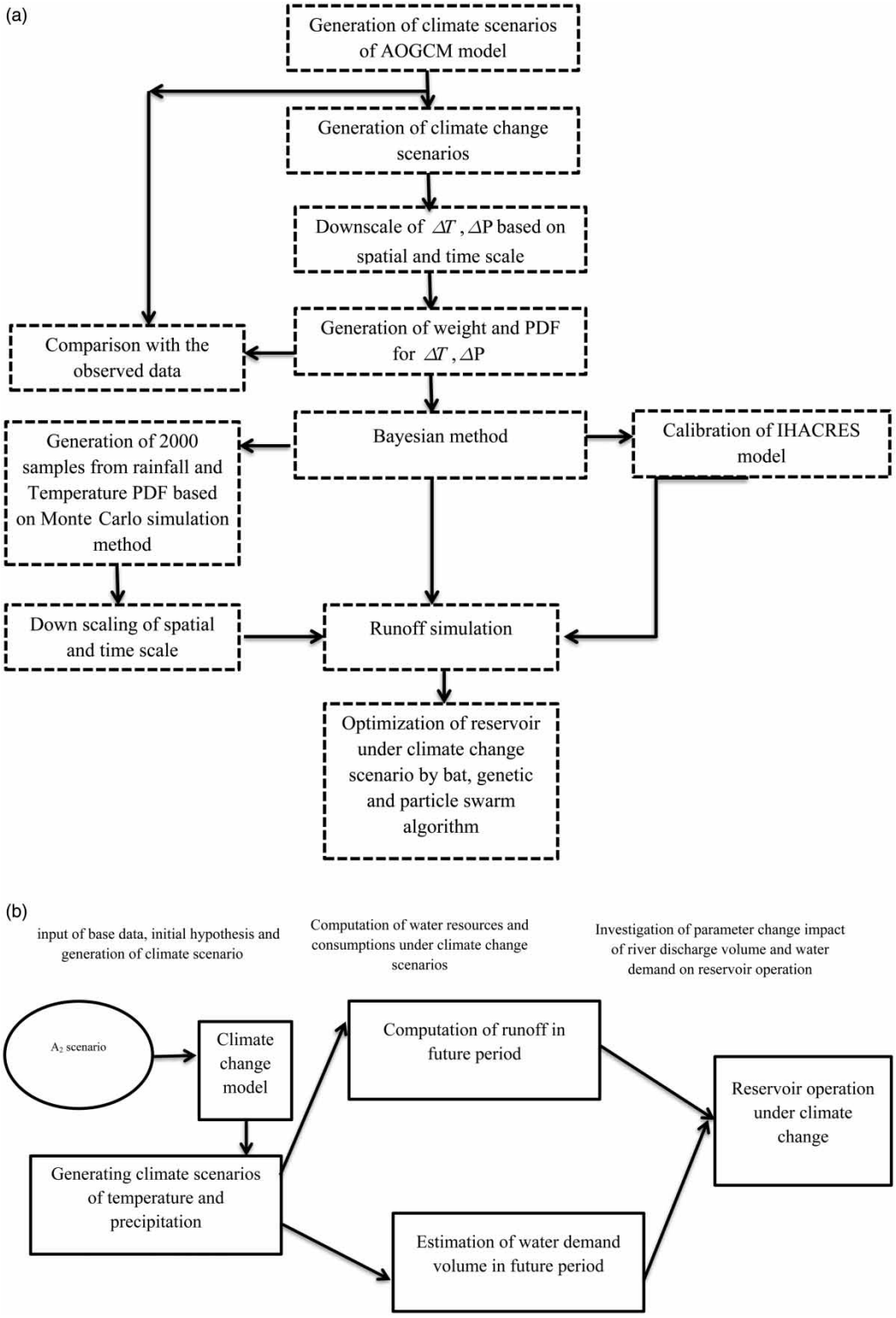

Figure 1 | (a) Methodology and (b) detail of reservoir operation under climate change condition.

decision-making was used to select the best method for reservoir operation in the base and future periods. The proposed model has been developed for Dez dam in Iran.

METHODOLOGY

General circulation model

Atmosphere-ocean general circulation models (AOGCMs) are used for the prediction of climate change under different scenarios. These models are based on physical laws expressed as mathematical equations. The five models of HAD-CM3, CGCM2, CSIRO-MK2, ECHAM4-OPY3, and GFDL-R30 are used for climate change prediction (IPCC-TGCIA 1999). Also, the A2 scenario is used for these models. This scenario emphasizes fast population growth and less dependence on economic advances based on family relations. Table 1 shows the spatial accuracy of different models (IPCC-TGCIA 1999). The AOGCM models use large-scale computational cells and simulate climate change according to noises. The average period data should be used instead of direct data. The climate change scenarios are generated based on the following equations:

$$\Delta T_i = \left(\bar{T}_{GCM,fut,i} - \bar{T}_{GCM,base,i}\right) \tag{1}$$

$$\Delta P_i = \left(\frac{\bar{P}_{GCM,fut,i}}{\bar{P}_{GCM,base,i}}\right) \tag{2}$$

where ΔT_i and ΔP_i: the climate change scenarios for temperate and precipitation, respectively, $\bar{T}_{GCM,fut,i}$: the simulated average of temperature for the period 2011–2030, and $\bar{T}_{GCM,base,i}$: the simulated average of temperature for the base period (1981–2000). Also, the precipitation parameters are defined as temperature parameters.

Different methods can be used as downscaling which decreases the scale of cells in comparison with time and spatial scale. The proportional method as a downscaling strategy for decreasing the spatial scale of cells is used in which climate variables are extracted from the cells of the location where the case study is located. The second method is related to another strategy which is known as change factor method to decrease the cell scale ratio to the time. The time climate change scenarios for the future period are computed by adding climate change scenarios to the observation values (1981–2000):

$$T = T_{obs} + \Delta T \tag{3}$$

$$P = P_{obs} + \Delta P \tag{4}$$

where T_{obs}: the time series of observation data in the base period, T: the time series of temperature for climate change in the future period (2011–2030), and ΔT: the downscaled climate change scenario.

IHACRES model for runoff simulation

This software is used for hydrological simulation and has two important modules. Nonlinear module converts observed precipitation to effective rainfall. Then, a linear unit hydrograph module converts the effective rainfall to runoff (Jakeman & Hornberger 1993). The wetness index is used for converting of rainfall to effective rainfall, based on the following equation:

$$u_k = s_k \times r_k \tag{5}$$

The wet index (s_k) is a function of evapotranspiration which is expressed as:

$$s_k = C \times r_k + \left(1 - \frac{1}{\tau_w(t_k)}\right) s_{k-1'} \tag{6}$$

$$\tau_w(t_k) = \tau_w e^{0.062f(R-t_w)} \tag{7}$$

Table 1 | Different climate change models

Model	GFDL-R30	CGCM2	CSIRO-MK2	ECHAM4-OPY3	HAD-CM3
Spatial accuracy (longitude × latitude) (degree)	4.5 × 7.5	3.7 × 3.7	3.2 × 5.6	2.8 × 2.8	2.5 × 3.75

where $\tau_w(t_k)$: an index for controlling of s_k when precipitation does not occur, R: the reference temperature, τ_w: the catchment drying time constant, and f: the temperature modulation factor.

First, the IHACRES module for the basin should be calibrated. Thus, observed temperature, discharge, and precipitation for the base period are used. Then, runoff volume of the basin for the period 2011–2030, based on temperature and precipitation input, is computed.

Uncertainty in climate change

There are different sources of uncertainty which are divided into the following groups:

1. uncertainty in AOGCM models for the simulation of climate change variables;
2. uncertainty in different downscaling methods;
3. uncertainty in runoff simulation methods.

In this study, the first kind of uncertainty was determined based on Bayesian strategy. The following levels were considered for the computation of uncertainty (Katz 2002):

1. A prior probability distribution was generated for statistical parameters.
2. The likelihood distribution of the observed data was determined as a function of parameters.
3. The posterior probability distribution was determined, based on the computed distribution of input data and the likelihood function.

First, the PDF of precipitation and temperature data was computed. Different weights were assigned to each model, based on the deviation of simulated precipitation and temperature from observed data and were computed as (Katz 2002):

$$R_i = \frac{1/B_{x,i}}{\sum_{i=1}^{N} B_{x,i}} \tag{8}$$

where $B_{x,i}$: the average difference of simulated temperature or precipitation for the base period in the x month with the average of observed data, N: the number of models, and R_i: the assigned weight to each model.

First, the PDF of climate change scenarios and monthly precipitation and temperature was computed and then the Monte Carlo method was used for the simulation of large data.

Modeling algorithms

The bat algorithm, genetic algorithm, and particle algorithms as powerful methods are considered for optimizing of reservoir operation with consideration of climate change condition. Thus, these methods are defined here based on the equation and mathematical models so that the process for each algorithm is defined in the following sections.

Bat algorithm

The bats act based on echolocation ability for finding food or identifying food from an obstacle. They generate loud sounds and these sounds return from the surroundings to the initial place of sound production and returning sounds have a specific pulse. Also, the generated pulses have different frequencies. The wavelength for each sound is computed as (Yang & Hossein Gandomi 2012):

$$\lambda = \frac{\upsilon}{f} \tag{9}$$

where υ: the speed of sound in the air, λ: the wavelength, and f: the frequency.

Also, the following assumptions were considered for the bat algorithm:

1. All bats applied the echolocation ability for finding of food and this ability allowed the bats to separate an obstacle from the food.
2. Each bat can search prey by a sound with the velocity (υ_i) at location (y_l) with frequency (f), wavelength (λ_i) and loudness (A_0).
3. The loudness can change from A_0 as a large constant value to a minimum value (A_{min}).

In addition, the frequency is in the domain of f_{min} and f_{max}. Also, the wavelength domain is between λ_{max} and λ_{min}. The emission rate of sound for each bat is r and it is between 0 and 1. Figure 2 shows the bat algorithm.

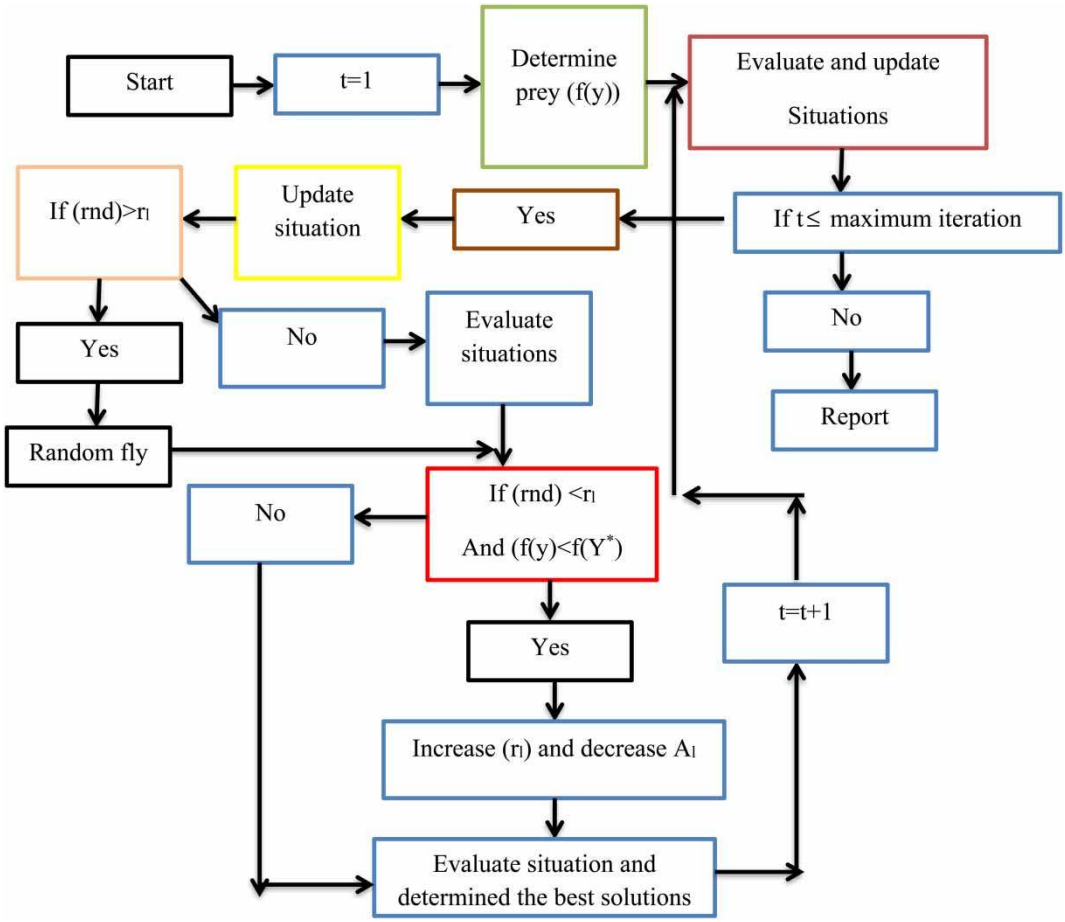

Figure 2 | Bat algorithm.

First, the frequency, velocity, and position should be updated based on the following equations:

$$f_l = f_{\min} + (f_{\max} - f_{\min}) \times \beta \tag{10}$$

$$v_l(t) = (y_l(t-1) - Y_*) \times f_l \tag{11}$$

$$y_l(t) = y_l(t-1) + v_l(t) \tag{12}$$

where $y_l(t-1)$: the position at time $t-1$, β: the random vector between 0 and 1, and $Y*$: the best position for bats (global solution).

Then, a random walk was considered for local search based on the following equation:

$$y(t) = y(t-1) + \varepsilon A(t) \tag{13}$$

where ε: the random number in the range of $[-1,1]$ and A(t): the average loudness.

When a bat finds its prey, the loudness decreases and the pulsation rate increases for each bat. The pulsation rate is updated based on the following equation:

$$r_l^{t+1} = r_l^0[1 - \exp(-\gamma t)]A_l^{t+1} = \alpha A_l^t \tag{14}$$

where α and γ are constant values.

The bat algorithm occupies the following levels:

1. Start.
2. The initial values of random parameters (y_l, v_l, f_l,….) should be determined.
3. The objective function for each bat position should be evaluated and the situation should be updated.
4. Then, the number of iterations should be compared with the maximum iterations and if it is equal or more than the

maximum iterations, results should be reported or else the next level should be done.
5. The situation should be updated.
6. The rnd as a random number should be compared with r_l and if it is more than r_l, the random fly should be considered or else the situations should be evaluated.
7. If rnd $<A_l$ and $f(y_l) < f(Y_*)$ are satisfied, evaluate the situation and determine the best solution.
8. Or else, the algorithm returns to the third level (Figure 2).

Genetic algorithm

The real genetic algorithm is used in optimization. The elitist level in this algorithm can keep the best members for the next generation. Then, the crossover operator is used to generate the better offspring. Also, the mutation operator is applied to add the diversity of the population. Two parents are used for generating children at the crossover level. Then, $Y^1 = \left(y_1^{(1)}, y_2^{(1)}, \ldots, y_n^{(1)}\right)$ and $Y^2 = \left(y_1^{(2)}, y_2^{(2)}, \ldots, y_n^{(2)}\right)$ are considered as parents and $X^1 = \left(x_1^{(1)}, x_2^{(1)}, \ldots, x_n^{(1)}\right)$ and $X^2 = \left(x_1^{(2)}, x_2^{(2)}, \ldots, x_n^{(2)}\right)$ are considered as children. Then, the polynomial distribution is considered for generating the γ parameter based on random parameter u:

$$\gamma = \begin{bmatrix} (\alpha u)^{1/(\eta_c+1)} \leftarrow \text{if}\left(u \le \dfrac{1}{\alpha}\right) \\ \left(\dfrac{1}{2-\alpha u}\right)^{1/(\eta_c+1)} \leftarrow \text{otherwise} \end{bmatrix} \tag{15}$$

where $\alpha = 2 - \beta^{-(\eta_c+1)}$ and β is computed as:

$$\beta = 1 + \frac{2}{x_i^{(2)} - x_i^{(1)}} \min\left[\left(x_i^{(1)} - x_i^{(l)}\right), \left(x_i^{(u)} - x_i^{(2)}\right)\right] \tag{16}$$

where the η_c parameter is considered as a distribution index. A small value of this parameter generates children far from the parents and a large value of this parameter generates children which are near to parents. The $x_i^{(1)}$ and $x_i^{(u)}$ are the lower and upper decision variables. The children are generated, based on the following equations:

$$\begin{aligned} y_i^{(1)} &= 0.5\left[\left(x_i^{(1)} + x_i^{(2)}\right) - \gamma\left|-x_i^{(1)} + x_i^{(2)}\right|\right] \\ y_i^{(2)} &= 0.5\left[\left(x_i^{(1)} + x_i^{(2)}\right) + \gamma\left|-x_i^{(1)} + x_i^{(2)}\right|\right] \end{aligned} \tag{17}$$

In the next level, the mutation operator is considered. $X = (x_1, x_2, \ldots, x_n)$ is considered as one of the parents and the mutated vector x_i from the X parent is considered based on the following equation:

$$x_i' = \begin{bmatrix} x_i + \Delta\left(t, x_i^u - x_i\right) \leftarrow (\tau = 0) \\ x_i + \Delta\left(t, x_i - x_i^l\right) \leftarrow (\tau = 1) \end{bmatrix} \tag{18}$$

where τ is the Boolean value. The function $\Delta(t, y)$ is computed as:

$$\Delta(t, y) = y\left(1 - r^{(1-(t/t_{\max}))^b}\right) \tag{19}$$

where r is the random number and t_{max} is the maximum iteration.

Particle swarm algorithm

The PSOA considers the particle velocity and position. If a D-dimensional search space is considered, the ith particle is based on the vector $X_i = (x_{i1}, x_{i2}, \ldots, x_{iD})^T$. The velocity for each particle is based on the vector $V_i = (v_{i1}, v_{i2}, \ldots, v_{iD})^T$. The best previous position for each particle is $P_i = (p_{i1}, p_{i2}, \ldots, p_{iD})^T$. Also, the g index is related to the best particle among other members. The position and velocity are updated based on the following equations:

$$v_{id}^{n+1} = \chi\left[w v_{id}^n + \frac{c_1 r_1^n\left(p_{id}^n - x_{id}^n\right)}{\Delta t} + \frac{c_2 r_2^n\left(p_{gd}^n - x_{gd}^n\right)}{\Delta t}\right] \tag{20}$$

$$x_{id}^{n+1} = x_{id}^n + \Delta t v_{id}^{n+1} \tag{21}$$

where χ: the constriction coefficient; w: the inertia weight, c_1 and c_2: the acceleration coefficients, and r_1 and r_2: the random numbers.

First, the initial velocity and position are generated. Then, the objective function is computed for each particle. The p best and g best as a local solution and global solution are computed in the next level. Then, the velocity and position are updated based on the previous formula.

Multi-criteria decision-making

The weighted aggregates sum product assessment (WASPAS) acts, based on the weighted sum model and the weighted product model. This module is useful when there are some methods and some indexes. For example, the reservoir operation is considered based on the bat algorithm, genetic algorithm, and particle swarm algorithm; and there are some indexes, such as reliability index, vulnerability index, resiliency index, and one objective function for each method. The best method can be selected when a multi-criteria decision is used by the user. If the f indexes are considered for the evaluation of each method and the value of each method for each index is considered based on the x_i value, the following levels are considered (Zavadskas *et al.* 2012):

1. Compute the normalized x for beneficial criteria and non-beneficial criteria. The indexes where a high percentage of them are suitable are named beneficial criteria and vice versa for non-beneficial criteria (Bozorg-Haddad *et al.* 2014).

$$\bar{x}_{ef} = \frac{x_{ef}}{Max(x_{ef})} \leftarrow (beneficial\_criteria) \tag{22}$$

$$\bar{x}_{ef} = \frac{Min(x_{ef})}{x_{ef}} \leftarrow (nonbeneficial\_criteria) \tag{23}$$

2. ϕ_e^1 and ϕ_e^2 are computed based on weights assigned to each index (Bozorg-Haddad *et al.* 2014):

$$\phi_e^1 = \sum_{f=1}^{n_c} \bar{x}_{ef} w_f \tag{24}$$

$$\phi_e^2 = \prod_{f=1}^{n_c} (\bar{x}_{ef})^{w_f} \tag{25}$$

In order to evaluate the proposed model, four indexes are considered, resiliency index, vulnerability index, reliability index, and objective function. In fact, these four indexes have the same priority and thus, the assigned weight (w_f) is equal to 0.25 for each index.

3. Finally, the total ϕ is computed as:

$$\phi = \lambda(\phi_e^1) + (1-\lambda)(\phi_e^2) \tag{26}$$

The range of λ is between 0 and 1. The ten intervals from 0 to 1 are considered for λ to see the variation of ϕ.

THE CASE STUDY

The Dez dam is known as the 50th highest dam in the world. This dam is located in the Andimeshk in south Iran (Figure 3). This is an arch dam and was constructed between 1953 and 1963. It is a multi-purpose dam and is used for flood control, irrigation water supply, and power generation; however, in this research, the focus is on the water supply for irrigation demand purposes because it has greater priority for decision-makers.

Dez dam characteristics

The irrigation supply in this study was important and the following objective function was considered for irrigation supply (Bozorg-Haddad *et al.* 2014):

$$\text{Minimize } (OF) = \sum_{t=1}^{T} \left(\frac{D_t - R_t}{D_{\max}}\right)^2 \tag{27}$$

where OF is the objective function, D_t the demand (MCM), R_t the water release, and D_{max} the maximum demand. The demand is set based on Equations (36)–(39).

The decision variable is the water release and the state variable is the dam storage.

The continuity equation was expressed as (Bozorg-Haddad *et al.* 2014):

$$S_{t+1} = S_t + Q_t - Loss_t - R_t - SP_t \tag{28}$$

where S_{t+1} is the storage at time $t+1$, Q_t is the inflow at time $t+1$, Loss_t is the losses value at time t, and SP_t is the overflow value at time t.

The losses value was computed as (Bozorg-Haddad *et al.* 2014):

$$Loss_t = A_t \times Ev_t \tag{29}$$

where A_t is the area of reservoir lake and Ev_t is the evaporation amount.

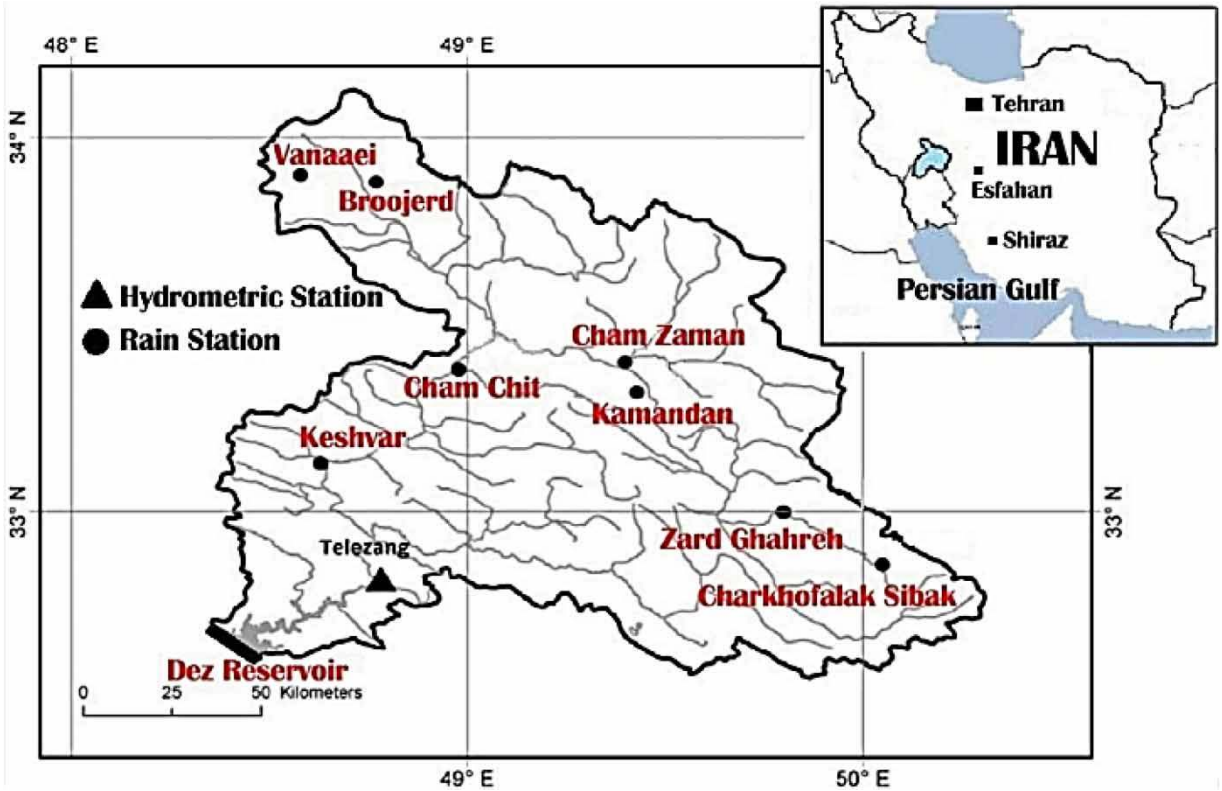

Figure 3 | Location of Dez Reservoir.

The overflow was computed based on the following equation (Bozorg-Haddad *et al.* 2014):

$$Sp_t = \begin{bmatrix} 0 \leftarrow if(S_t \leq S_{\max}) \\ S_{\max} - S_t \leftarrow if(S_t > S_{\max}) \end{bmatrix} \tag{30}$$

where S_{max} is the maximum storage for the reservoir.

Also, the following constraints were considered for this reservoir (Bozorg-Haddad *et al.* 2014):

$$0 \leq R_t \leq D_t \tag{31}$$

$$S_{\min} \leq S_t \leq S_{\max} \tag{32}$$

Three penalty functions are considered for the reservoir (Bozorg-Haddad *et al.* 2014):

$$P_{1,t} = \begin{bmatrix} 0 \leftarrow if(S_{t+1}) > S_{\min} \\ \left(\dfrac{(S_{\min} - S_{t+1})^2}{S_{\min}}\right) \end{bmatrix} \tag{33}$$

$$P_{2,t} = \begin{bmatrix} 0 \leftarrow if(S_{t+1} < S_{\max}) \\ \left(\dfrac{(S_{t+1} - S_{\max})^2}{S_{\max}}\right) \leftarrow \text{otherwise} \end{bmatrix} \tag{34}$$

$$P_{3,t} = \begin{bmatrix} 0 \leftarrow if(R_t < D_t) \\ \left(\dfrac{(R_t - D_t)^2}{D_{\max}}\right) \leftarrow \text{otherwise} \end{bmatrix} \tag{35}$$

The penalty function was added to the objective function.

Computation of water demand for reservoir downstream

First, the crop coefficient and reference crop evapotranspiration were considered for the computation of crop evapotranspiration as (Ashofteh *et al.* 2017a):

$$ET_C = K_{C_t} \times ET_0 \tag{36}$$

where ET_C is the crop evapotranspiration, K_{C_t} is the crop coefficient, and ET_0 is the reference crop evapotranspiration.

The Soil Conservation Service (SCS) method was used for the computation of effective rainfall based on the following equations (Ashofteh *et al.* 2017a):

$$P_{eff_t} = \frac{P_t}{125} \times (125 - 0.2P_t) \leftarrow P_t \leq 250\text{mm}$$
$$P_{eff_t} = 125 + 0.1 \times P_t \leftarrow P_t \geq 250\text{mm} \quad (37)$$

where P_{eff_t} is the effective rainfall.

Equation (37) shows the volume of net water requirement (Ashofteh *et al.* 2017a):

$$WR_t = ET_{C_t} - P_{eff_t} \quad (38)$$

where WR_t is the net water requirement.

The demand volume was computed as (Ashofteh *et al.* 2017a):

$$V_t = \frac{WR_t \times 10 \times A}{1,000,000} \quad (39)$$

There are four main agriculture crops including forage, wheat, barley, and feed corn in the basin. Annual water requirement at a particular time (WR_t) for each crop in the base period is measured. For example, the water requirement for forage, wheat, barley, and feed corn is 1,555.12, 424.23, 769, and 1,234 mm, respectively. Subsequently, the future demand for each crop could be computed based on Equation (39). Usually, the WR_t is computed based on crop reference evapotranspiration. If the reference evapotranspiration is unavailable, this parameter will be computed based on a regression equation between temperature and evapotranspiration. On the other hand, K_{C_t} parameter should be computed in the next stage. Therefore, the relative humidity, wind speed, and the length of germination periods should be computed first. Sequentially, K_{C_t} is computed and then, ET_C is computed based on Equation (36), where V is the demand volume and A is the area under cultivation.

Also, the following indexes were used for evaluation of different methods.

1. Reliability index:

This index acts based on the ratio of the volume of water released in the total period to the total demand as (Ashofteh *et al.* 2017a):

$$\alpha_V = \frac{\sum_{i=1}^{T} R_{i,t}}{\sum_{i=1}^{T} D_{i,t}} \quad (40)$$

where α_V: the reliability index, D: the demand, and R: the water release.

2. Vulnerability index:

This index acts based on the intensity of system failure events:

$$\gamma = Max\left(\frac{D_t - R_t}{D_t}\right) \quad (41)$$

where γ is the vulnerability index.

3. Resiliency index:

This index shows the existence of the system from failure (Ashofteh *et al.* 2017a):

$$\gamma = \frac{f_s}{F_i} \quad (42)$$

where f is the number of series failure occurrence events, and F the number of failure events. In fact, the failure periods mean that there is a critical period that experienced drought period or water deficits. Thus, γ determines the effectiveness of the system operation against the number of failure events.

Also, the following indexes were used for the evaluation of climate change models.

1. Correlation coefficient:

$$r = \frac{1/n \sum_{m=1}^{n} (X_s - \mu_s)(X_o - \mu_o)}{\sigma_s \times \sigma_o} \quad (43)$$

$$RMSE = \sqrt{\sum_{i=1}^{n} \frac{(X_s - X_o)^2}{n}} \quad (44)$$

$$MAE = \frac{\sum_{m=1}^{n} |X_s - X_o|}{n} \quad (45)$$

where r: the correlation coefficient, n: the number of data, X_s: the simulated data, X_o: the observed data, μ_s the simulated average, μ_o: the observed average, σ_s: the standard deviation for simulated data, RMSE: the root mean square error, and MAE: the mean absolute error.

RESULTS AND DISCUSSION

Temperature and precipitation for the base period

First, daily temperature and rainfall based on climatology stations of Dez basin were completed for the AOGCM models for the temperature and precipitation simulation. Then, monthly temperature and precipitation data of AOGCM models were

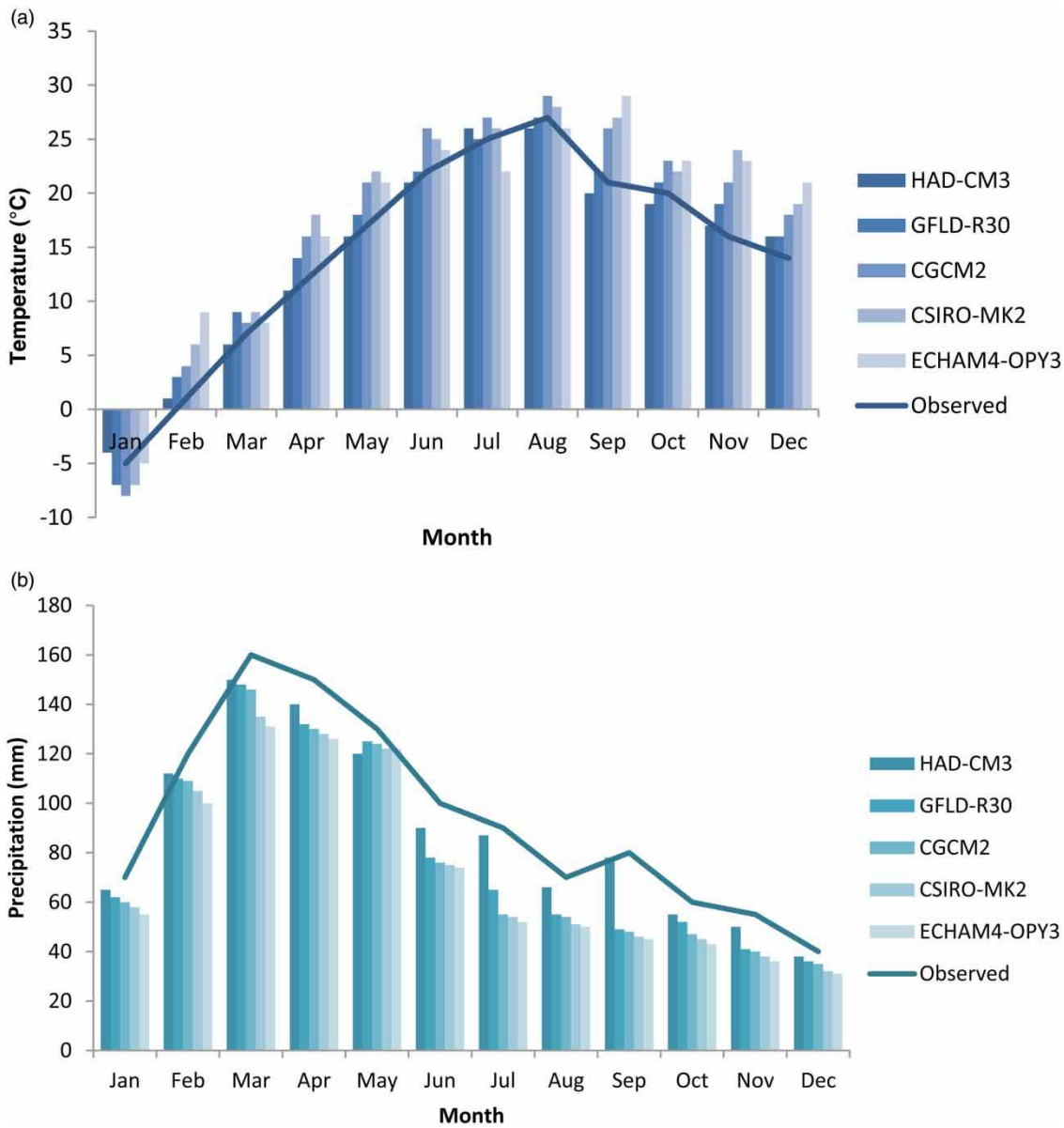

Figure 4 | (a) Simulated temperature for the base period and (b) simulated precipitation for the base period.

extracted from the IPCC base which included time series of climate variables of computational cells (IPCC-DDC 1999). Then, the monthly average of 20 years (1981–2000) was computed and these values were compared with observed values. In this study, the GCM-RDP program was used for the extraction of time series, because this program can obtain the time series after receiving the spatial coordinates of the location of a case study (Nezhad *et al.* 2013).

Figure 4 shows the performance of different climate change models and compares results with observed data. The HAD-CM3 model yielded the average temperature for the base period as 14.58°C which was close to the observed temperature of 14.75°C. Table 2 also shows this closeness based on statistical indexes. The correlation coefficient for HAD-CM3 model was 97% and MAE and RMSE had small values which showed the high performance of the HAD-CM3 model. Figure 4 shows simulated precipitation for the base period with different climate change models. The observed average precipitation for the base period was 93.75 mm and the simulated value based on HAD-CM3 model was 91.25 mm, again showing the HAD-CM3 model performed well for precipitation simulation. Table 2 shows small values of MAE and RMSE based on the HAD-CM3 model and the correlation coefficient (r) was high for the simulated precipitation.

Table 2 | Statistical analysis for temperature and precipitation (base period)

Temperature

Parameter	MAE (°C)	RMSE (°C)	r%
HAD-CM3	2.00	3.00	97
CGCM2	3.00	4.00	92
CSIRO-MK2	3.51	4.55	93
GFLD-R30	3.76	5.00	92
ECHAM-OPY3	3.96	5.51	90

Precipitation

Parameter	MAE (mm)	RMSE	r%
HAD-CM3	1	1.5	98
CGCM2	3	2.5	96
CSIRO-MK2	5	5.5	94
GFLD-R30	6	6.25	90
ECHAM-OPY3	6.5	6.90	89

Temperature and precipitation for future period

First, monthly temperature and precipitation were downscaled under the A2 scenario. Then, the average

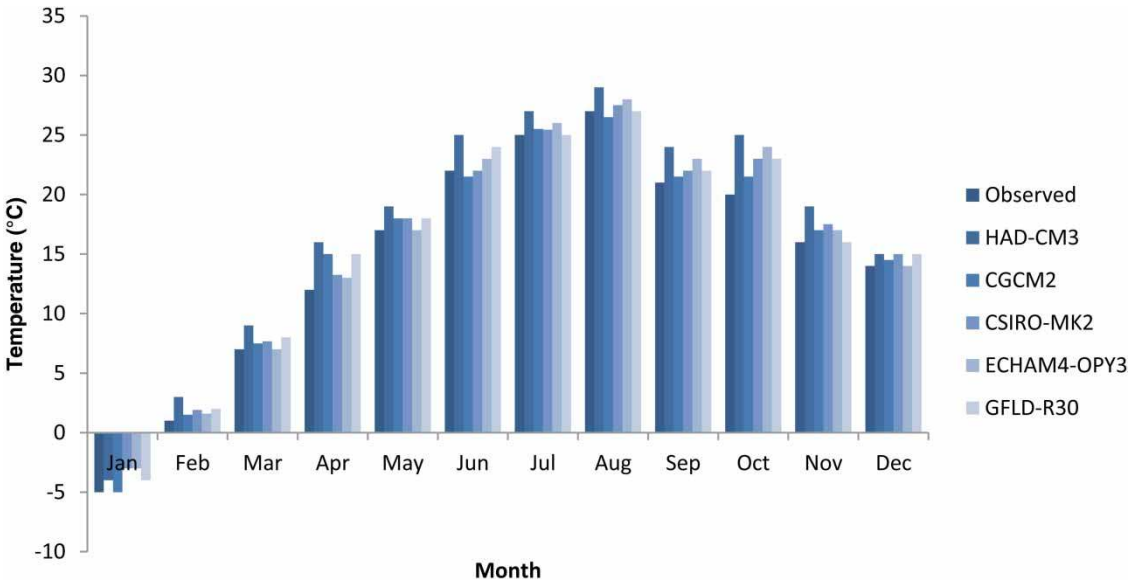

Figure 5 | The simulated temperature for the future period.

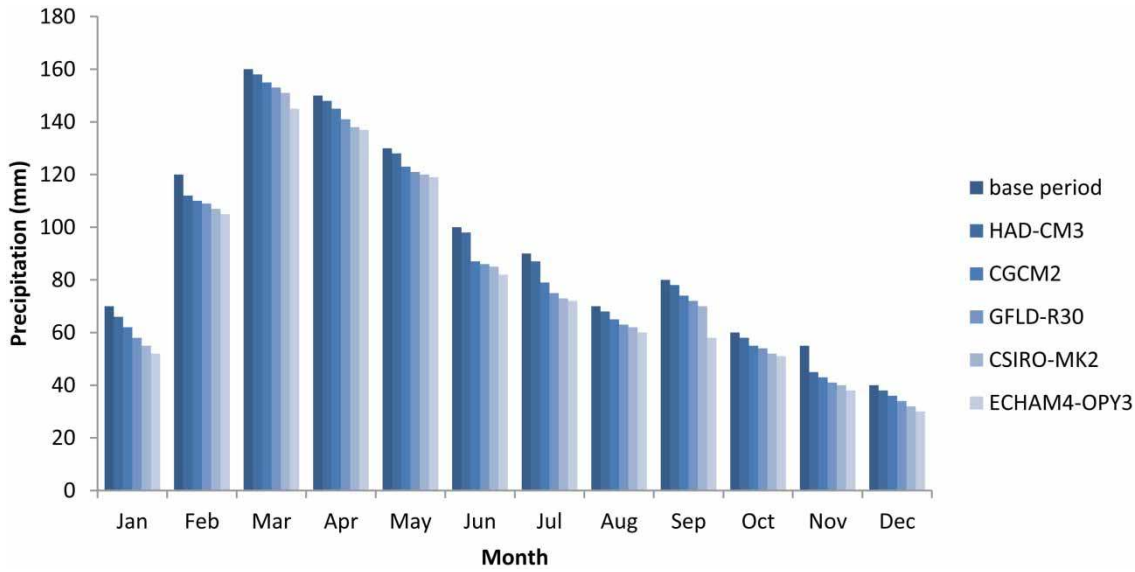

Figure 6 | The simulated precipitation for the future period.

monthly temperature and precipitation for a long period were simulated for the base and future periods. Simulated temperature for the future period in Figure 5 shows that the temperature is increasing from 1.16 to 2.5°C compared to the base period. The ECHAM4-OPY and GFLD-R30 model had predicted the least value of temperature increase for the future period and the HAD-CM3 model had predicted the greatest value of temperature increase for the future period. Also, Figure 6 shows the simulated precipitation for the future period and it had decreased from 3.33 mm compared to 9 mm for the base period. The ECHAM4-OPY3 and CSIRO-MK2 models had predicted the greatest value of precipitation decrease for the future period. Also, the HAD-CM3 model had predicted the least value of precipitation decrease for the future period. Figures 5 and 6 show the average monthly precipitation for the long term (20 years).

Computation of uncertainty among different climate change models

Figure 7 shows the computed weights for different climate change models. Each model based on the Bayesian equation (Equation (8)) had a weight and then the monthly PDFs of temperature and precipitation were computed. The HAD-CM3 model had the most weight for temperature and precipitation, whereas the CSRI-MK2 model had the least weight. Thus, the HAD-CM3 model had the most effect on temperature and precipitation in the region. The scenario of climate change of temperature and precipitation from each PDF was selected after determining the PDF of climate change scenario for the region based on Mont Carlo simulation.

Runoff simulation for the base and future period

Figure 8 shows runoff simulation for the base and future periods. The correlation coefficient for calibration data was 91% and 87% for verification data. Also, MAE and RMSE were 1.25 and 2.12 m^3/s, respectively, for calibration and were 1.87 and 3.45 m^3/s for verification, respectively. Figure 9 shows discharge for the base and future periods and runoff volume had decreased by $0.05 \times 10^6\ m^3$ for the future period. The period between the years 1981 and 1992 is considered for the calibration model and the period between the years 1993 and 2000 is considered for model verification.

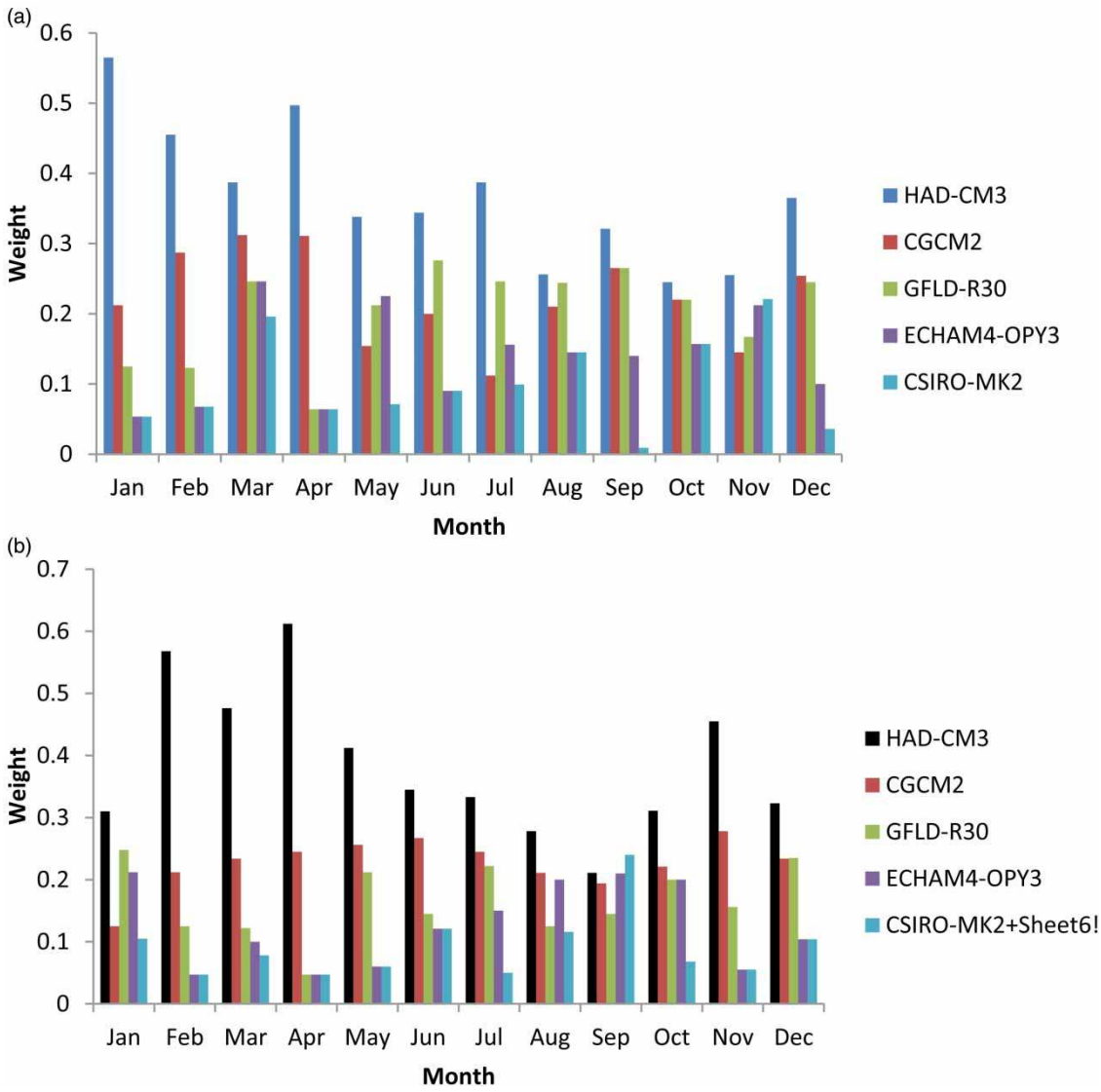

Figure 7 | (a) Assigned weight for temperature and (b) assigned weight for precipitation.

Computation demand for the future periods

Computation of demand for the future period needed some information which was not available for the future period. First, a relationship between temperature and reference evapotranspiration based on the base period was extracted for use for the future period. This relationship was based on regression with a high correlation coefficient ($R^2 = 0.90$). Then, ET_0 was computed, based on the previous relationship after temperature was computed for the future period. Also, the K_C coefficient was computed based on each crop for the future period. Then, Equation (35) was used for evapotranspiration of crop. Finally, the demand volume was computed based on the previous equations. Table 3 shows the demand value for each crop. The increase of demand for different crops was from 0.55 to $1.63 \times 10^6\,m^3$ and Figure 10 shows the demand value for the base and future periods so that it is clear that the demand volume had increased for the future period. In fact, Figure 10 shows the computed water requirement for 20 years in future based on Equation (39) and it is compared with the observed value.

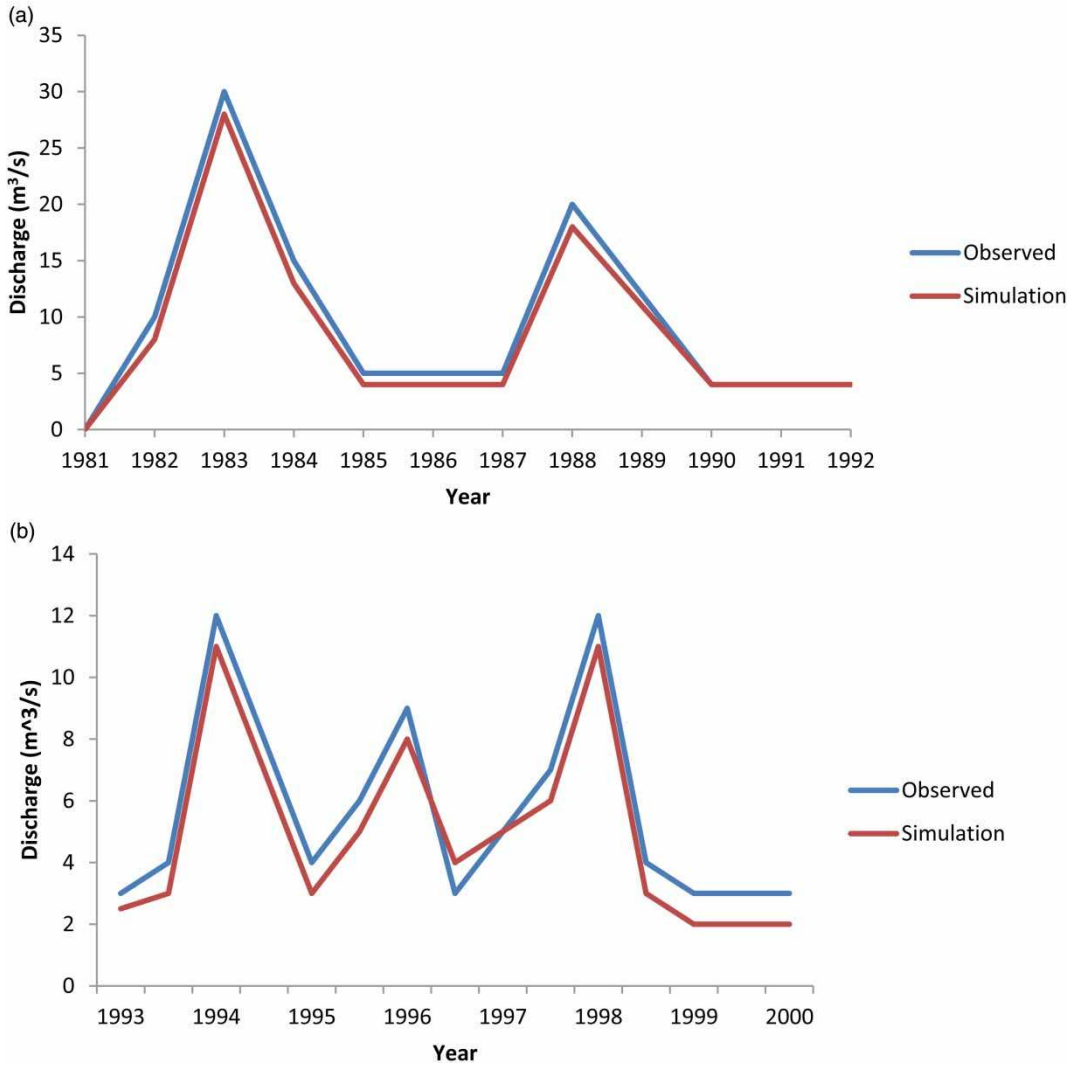

Figure 8 | (a) Calibration model for runoff simulation and (b) verification model for runoff simulation.

Sensibility analysis for evolutionary algorithms

Table 4 shows the sensibility analysis for different evolutionary algorithms for the base and future period. The size population for the bat algorithm is 30 and 50 for the base and future period. Also, maximum loudness is 0.6 for the base and future period. The maximum frequency is 5 for the base and future period. In fact, the least value of objective function is searched in Table 4 and the corresponding parameter for this value of objective function is selected. Also, the other parameter for the other evolutionary algorithms can be seen in Table 4. In fact, the sensibility analysis shows the change of the objective function versus the change of different variables and then the suitable value for each variable is selected.

Ten random results for evolutionary algorithms and convergence curves

Table 5 shows ten random results for different algorithms and the following can be seen:

1. The average result for the bat algorithm was less than that for the genetic algorithm and particle swarm algorithm for the base and future periods.

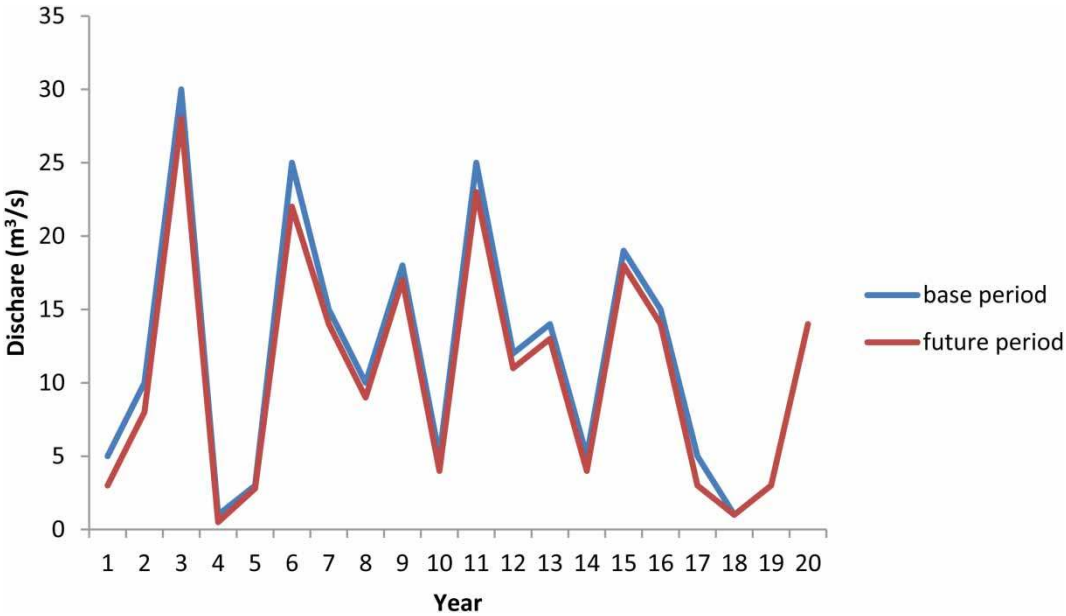

Figure 9 | Runoff simulation for the base and future periods.

Table 3 | Water demand for base and future periods

Crops	Area under cultivation (ha)	WR^a_{base} (mm)	WR^b_{future}	WR_{future}/WR_{base}	V^c_{base} (*10^6 m^3)	V^d_{future} (*10^6 m^3)	ΔV
Forage	970	1,555.12	1,654.23	1.06	15.38	16.34	0.96
Wheat	1,340	424.23	545.72	1.28	5.68	7.31	1.63
Barley	998	769	824	1.07	7.67	8.22	0.55
Feed corn	870	1,234	1,345	1.08	10.73	11.70	0.97

[a]Annual water requirement in base period.
[b]Annual water requirement in future period.
[c]Water demand volume in base period.
[d]Water demand volume in future period.

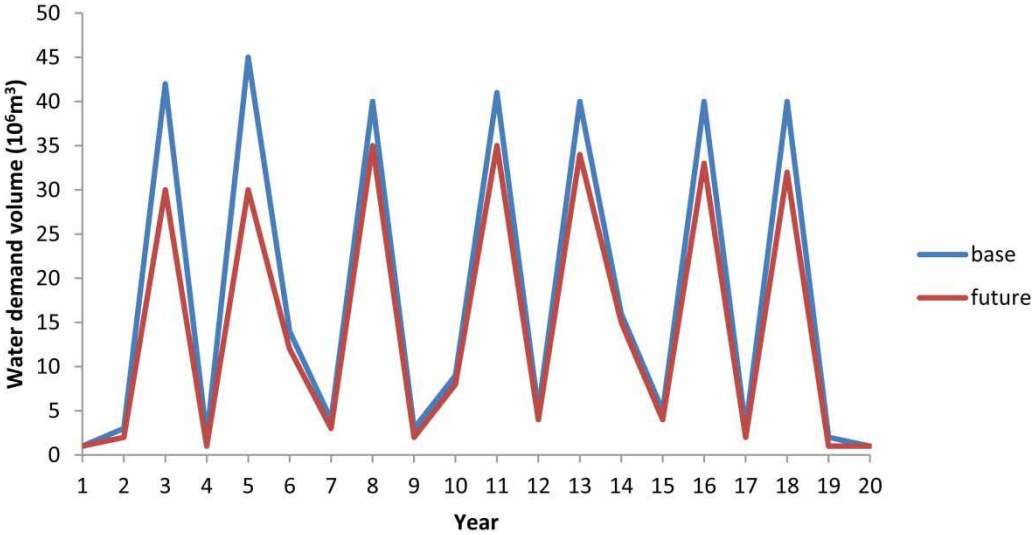

Figure 10 | Water demand for the base and future periods.

Table 4 | Sensibility analysis for evolutionary algorithms

(a)

Population	Objective function	Maximum loudness	Objective function	Maximum freqency	Objective function
Base period					
10	2.44	0.20	2.39	1	2.44
30	1.98	0.40	1.87	3	1.54
50	1.54	0.60	1.54	5	1.69
70	1.76	0.80	1.89	7	1.71
Future period					
10	4.23	0.20	4.45	1	4.12
30	3.11	0.40	3.01	3	2.77
50	2.76	0.60	2.75	5	3.12
70	2.87	0.80	2.92	7	3.24

(b)

Population	Objective function	$C_1 = C_2$	Objective function	Inertia weight	Objective function
Base period					
20	3.26	1.8	3.14	0.20	3.11
40	2.98	1.9	3.00	0.40	2.98
60	3.11	2.0	2.98	0.60	3.01
80	3.20	2.1	3.01	0.80	3.04
Future period					
20	5.12	1.8	5.10	0.20	5.09
40	4.98	1.9	5.00	0.40	4.98
60	4.77	2.0	4.98	0.60	5.12
80	4.89	2.1	5.01	0.80	5.14

(c)

Population	Objective function	Crossover probability	Objective function	Mutation probability	Objective function
Base period					
10	4.45	0.20	4.34	0.10	4.54
30	3.78	0.40	3.79	0.30	3.89
50	3.89	0.60	3.81	0.50	3.79
70	3.95	0.80	3.89	0.70	3.81
Future period					
10	6.23	0.20	6.12	0.10	6.12
30	5.11	0.40	5.11	0.30	5.87
50	5.44	0.60	5.34	0.50	5.44
70	5.89	0.80	5.54	0.70	5.74

2. The average solution for the genetic algorithm was worse than for the particle swarm algorithm and the bat algorithm for the base and future periods.
3. The coefficient of variation for the bat algorithm was smaller than for the genetic algorithm and particle swarm algorithm for the base and future periods.

Table 5 | Ten random results for evolutionary algorithms

Run	Bat algorithm	Particle swarm algorithm	Genetic algorithm
Base period			
1	1.54	2.99	3.95
2	1.55	2.98	3.89
3	1.54	2.99	3.95
4	1.54	2.98	3.89
5	1.55	2.98	3.89
6	1.54	3.05	3.89
7	1.54	2.98	3.89
8	1.54	2.98	3.89
9	1.54	2.98	3.89
10	1.54	2.98	3.89
Average	1.54	2.98	3.89
Variation coefficient	0.002	0.005	0.008
Future period			
1	2.77	4.83	5.45
2	2.76	4.77	5.11
3	2.76	4.80	5.45
4	2.76	4.77	5.45
5	2.76	4.77	5.45
6	2.76	4.77	5.45
7	2.76	4.77	5.45
8	2.76	4.77	5.45
9	2.76	4.77	5.45
10	2.76	4.77	5.45
Average	2.76	4.77	5.45
Variation coefficient	0.002	0.003	0.019

4. Results for the base period for all algorithms were less than for the future period.

Figure 11 shows the convergence for different algorithms. It can be seen that the bat algorithm converged in a fewer number of iterations than the particle swarm and genetic algorithms for the base period and future periods. The main indicator that the algorithm achieved the global solution is that the convergence curve becomes stable.

Water release for the base and future periods

Figure 12 shows the water released for the base and future periods for different algorithms. The average water volume released for the base period for the bat algorithm was 16.5 ($10^6\,m^3$), while it was 15 ($10^6\,m^3$) for the future period. The water volume released for the base period for the particle swarm algorithm was 14.65 ($10^6\,m^3$) and was 13.1 ($10^6\,m^3$) for the future period. The water volume released for the base period for the genetic algorithm was 13.25 ($10^6\,m^3$) and it was 103.5 ($10^6\,m^3$) for the future period. Thus, there were two general results:

1. The water volume released for the future period for the all algorithms was more than for the base period.
2. The released water volume for the bat algorithm for the future and base periods was more than for the genetic and particle swarm algorithm.

Thus, the bat algorithm can meet demand for the future and base periods better than the other algorithms.

Analysis based on different indexes

Table 6 shows the performance of different algorithms for reservoir operation. The reliability index for the base and future periods was more for the bat algorithm than for the particle swarm algorithm and genetic algorithm. Thus, the reservoir can meet demand based on the bat algorithm better than based on the other two algorithms. Also, the vulnerability index for the bat algorithm for the base and future periods is less than for the other two algorithms. The resiliency index for the particle swarm algorithm for the base and future periods was more than for the genetic algorithm and the bat algorithm and the objective function for the bat algorithm had a better value than for the genetic algorithm and particle swarm algorithm.

Table 7 shows the value of ϕ^1 and ϕ^2. Also, Table 8 shows the ϕ value for different values of $\lambda 2$. It is clear that the bat algorithm had greater value ϕ for all intervals of λ than had the genetic algorithm and particle swarm algorithm. Also, the Copeland procedure was used to

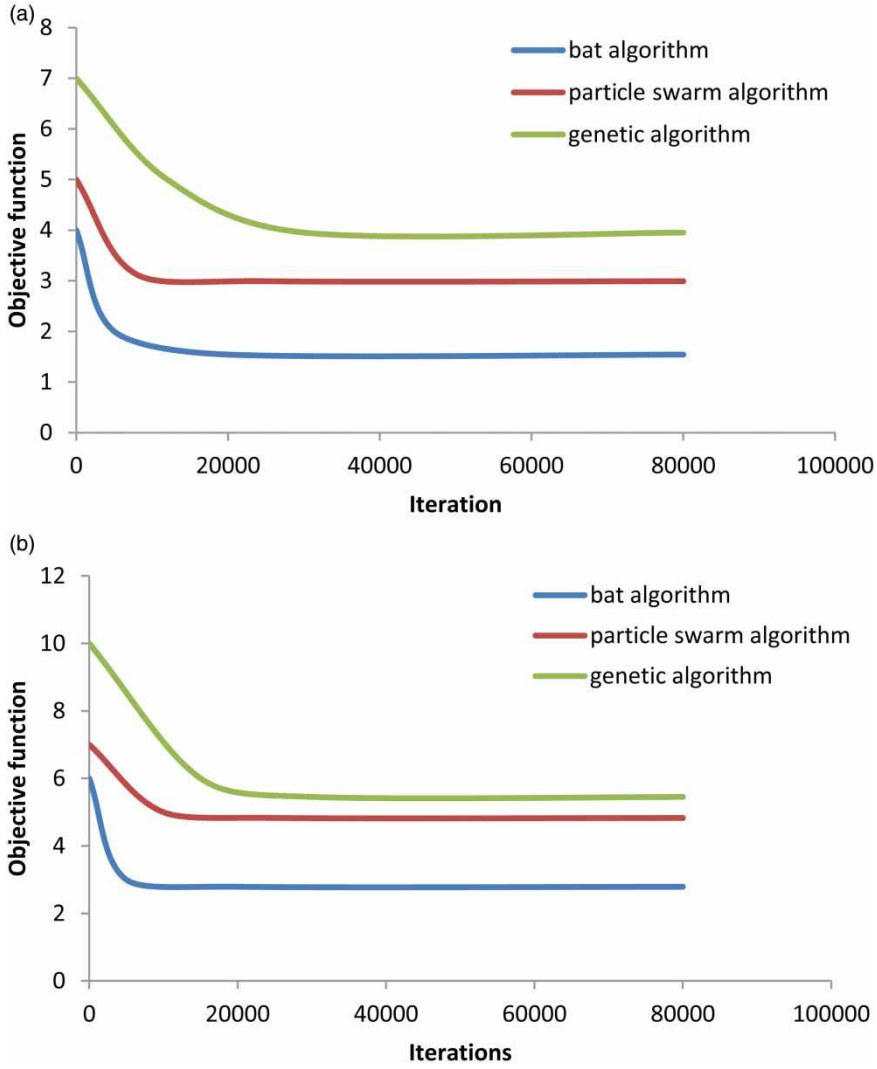

Figure 11 | Convergence curve for the (a) base period and (b) future period.

compare different methods among each other. Table 9 shows that the bat algorithm based on 11 intervals for λ had won compared to the genetic algorithm and particle swarm algorithm and, finally, Table 10 shows the superior status of the bat algorithm to the other methods.

CONCLUDING REMARKS

In this study, reservoir operation for irrigation demand supply was considered and reservoir operation under climate change based on different climate change models was investigated. The study of climate change models showed that the temperature of Dez basin in Iran would increase for the period 2011–2030 and precipitation would decrease for this period. Also, the Bayesian method was used to determine the more reliable climate change model whose results showed the HAD-CM3 model had more weight than the other models for temperature and precipitation. Also, the IHACRES software based on A2 scenario and the HAD-CM3 model were used for runoff simulation and statistical results showed the high performance of the

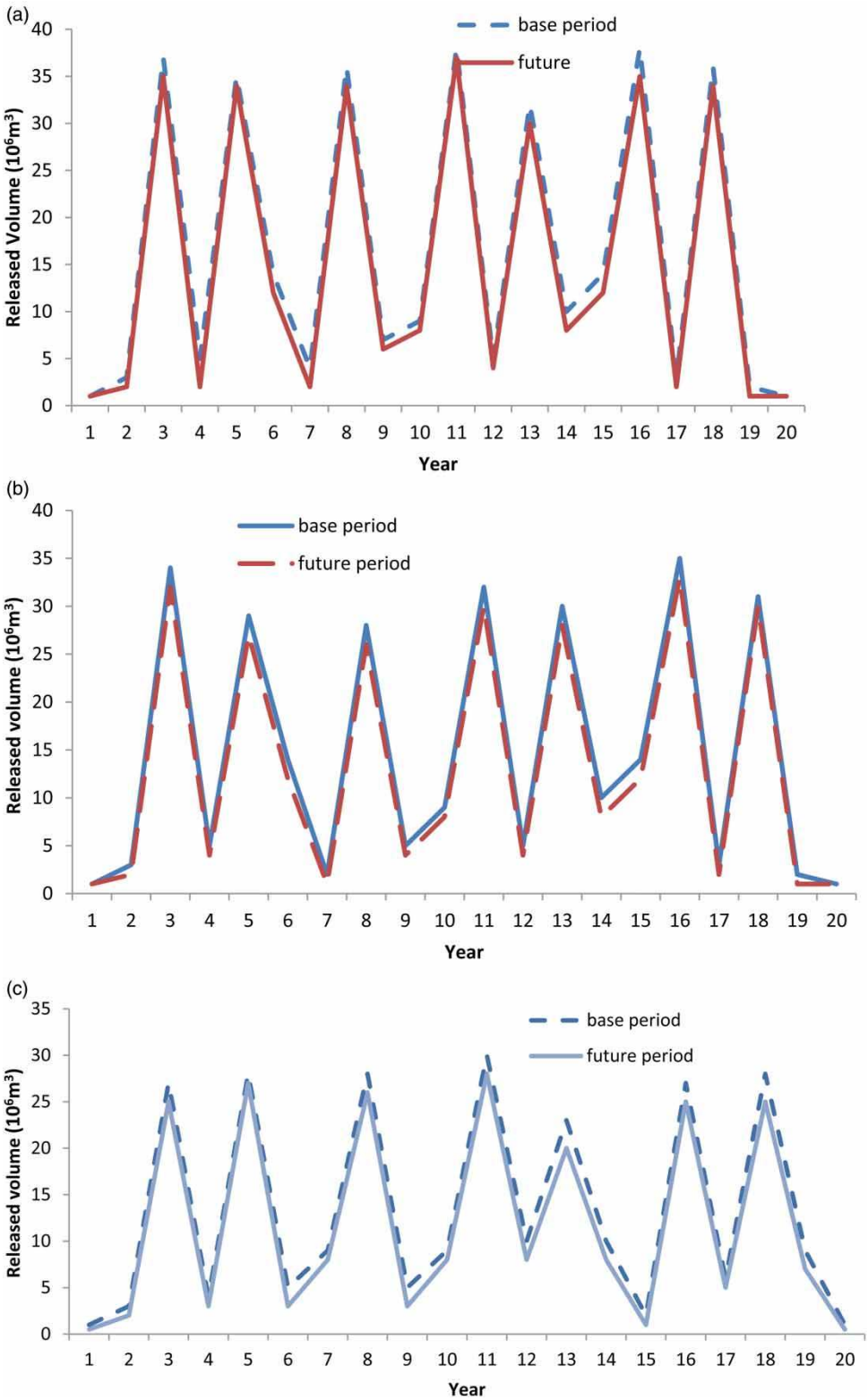

Figure 12 | The released water for (a) bat algorithm, (b) particle swarm algorithm and (c) genetic algorithm.

Table 6 | Different indexes for reservoir operation

Method	Reliability index %	Vulnerability index %	Resiliency index %	Objective function
Base period				
Decision matrix				
Bat algorithm	98	12	34	1.54
Genetic algorithm	90	16	29	3.95
Particle swarm algorithm	94	14	36	2.99
Normalized decision matrix				
Bat algorithm	1	1	0.94	1
Genetic algorithm	0.91	0.75	0.80	0.38
Particle swarm algorithm	0.95	0.85	1	0.51
Future period				
Decision matrix				
Bat algorithm	92	16	27	2.77
Genetic algorithm	80	25	22	5.45
Particle swarm algorithm	86	21	30	4.83
Normalized decision matrix				
Bat algorithm	1	1	0.90	1
Genetic algorithm	0.86	0.64	0.73	0.50
Particle swarm algorithm	0.93	0.76	1	0.57

Table 7 | Values of ϕ^1 and ϕ^2 for each algorithm

Parameter	Bat algorithm	Particle swarm algorithm	Genetic algorithm
Base period			
ϕ^1	0.985	0.71	0.8225
ϕ^2	0.983	0.67	0.801
Future period			
ϕ^1	0.975	0.6825	0.815
ϕ^2	0.974	0.6690	0.791

hydrological model. The results showed that the runoff volume would decrease by about $0.05 \times 10^6\,m^3$ for the future period compared to the base period and the predicted demand for the future period would be more than for the base period. The evolutionary algorithms for the future period yielded greater values than for the base period and the value of objective function for the bat algorithm for the future and base periods was less than for the other methods. The water volume released for all the evolutionary algorithms for the base period was more than for the future period and the bat algorithm for the future and base periods released more volume of water than did the particle swarm algorithm and genetic algorithm. Also, the WASPAS model showed that the bat algorithm was a better tool for reservoir operation than the genetic algorithm and particle swarm algorithm. In fact, the operation rule achieved by the bat algorithm could supply water demands better than the other algorithms based on different indexes such as reliability, vulnerability, and resiliency index. For example, the bat algorithm had the highest value of the reliability index compared to the other algorithms. Such observation reflects that the bat algorithm could introduce the highest stable operation rule with the best performance. The proposed model introduced in this article could be effective in the area of studying the influence of climate change on water resource management and planning. In fact, climate

Table 8 | Performance of each algorithm for different values of λ for (a) base period and (b) future period

Values	ϕ_{bat}	$\phi_{particle(algorithm)}$	$\phi_{genetic(algorithm)}$
(a) Base period			
$\lambda = 0$	0.9830	0.6700	0.8010
$\lambda = 0.10$	0.9832	0.6741	0.8030
$\lambda = 0.20$	0.9834	0.6780	0.8053
$\lambda = 0.30$	0.9836	0.6820	0.8074
$\lambda = 0.40$	0.9838	0.6860	0.8096
$\lambda = 0.50$	0.9840	0.6900	0.8117
$\lambda = 0.60$	0.9842	0.6940	0.8139
$\lambda = 0.70$	0.9844	0.6980	0.8160
$\lambda = 0.80$	0.9846	0.7020	0.8182
$\lambda = 0.90$	0.9848	0.7060	0.8230
$\lambda = 1.00$	0.985	0.7100	0.8225
(b) Future period			
$\lambda = 0$	0.9740	0.6690	0.7910
$\lambda = 0.10$	0.9741	0.6703	0.7934
$\lambda = 0.20$	0.9742	0.6717	0.7958
$\lambda = 0.30$	0.9743	0.6730	0.7982
$\lambda = 0.40$	0.9744	0.6744	0.8006
$\lambda = 0.50$	0.9745	0.6757	0.8030
$\lambda = 0.60$	0.9746	0.6771	0.8054
$\lambda = 0.70$	0.9747	0.6784	0.8078
$\lambda = 0.80$	0.9748	0.6798	0.8102
$\lambda = 0.90$	0.9749	0.6811	0.8126
$\lambda = 1.00$	0.9750	0.6825	0.8150

Table 9 | Pairwise contents based on Copeland procedure

Contender A	Contender B	Number of victories for A	Number of victories for B	Winner
Bat	Particle swarm	11	0	Bat
Bat	Genetic algorithm	11	0	Bat
Particle swarm	Genetic algorithm	11	0	Particle swarm

Table 10 | Final ranks based on Copeland procedure

Method	Rank
Bat algorithm	1
Particle swarm algorithm	2
Genetic algorithm	3

change is one of the major reasons for several real water scarcity occurrences around the world. Thus, the research contribution of this article could be of vital importance for developing water resource management concepts under climate change condition.

ACKNOWLEDGEMENTS

The authors are grateful for the financial support received from the University of Malaya Research Grant (UMRG) coded RP025A-18SUS University of Malaya, Malaysia.

REFERENCES

Agarwal, A. & Singh, R. D. 2004 Runoff modelling through back propagation artificial neural network with variable rainfall-runoff data. *Water Resources Management* **18** (3), 285–300.

Ahmadi, M., Haddad, O. B. & Mariño, M. A. 2014 Extraction of flexible multi-objective real-time reservoir operation rules. *Water Resources Management* **28** (1), 131–147.

Ahmadianfar, I., Adib, A. & Salarijazi, M. 2015 Optimizing multireservoir operation: hybrid of bat algorithm and differential evolution. *Journal of Water Resources Planning and Management* **142** (2), 05015010.

Alfieri, L., Perona, P. & Burlando, P. 2006 Optimal water allocation for an alpine hydropower system under changing scenarios. *Water Resources Management* **20** (5), 761–778.

Asgari, H. R., Bozorg Haddad, O., Pazoki, M. & Loáiciga, H. A. 2015 Weed optimization algorithm for optimal reservoir operation. *Journal of Irrigation and Drainage Engineering* **142** (2), 04015055.

Ashofteh, P. S., Rajaee, T. & Golfam, P. 2017a Assessment of water resources development projects under conditions of climate change using efficiency indexes (EIs). *Water Resources Management* **31**, 3723–3744.

Ashofteh, P. S., Bozorg-Haddad, O. & Loáiciga, H. A. 2017b Logical genetic programming (LGP) development for irrigation water supply hedging under climate change conditions. *Irrigation and Drainage* **66** (4), 530–541.

Ashofteh, P. S., Bozorg-Haddad, O. & Loáiciga, H. A. 2017c Development of adaptive strategies for irrigation water demand management under climate change. *Journal of Irrigation and Drainage Engineering* **143** (2), 04016077.

Beermann, J. 2017 Introduction. In: *Urban Cooperation and Climate Governance*. J. Lim (ed.). Springer Fachmedien, Wiesbaden, pp. 17–27.

Bozorg-Haddad, O., Karimirad, I., Seifollahi-Aghmiuni, S. & Loáiciga, H. A. 2014 Development and application of the bat algorithm for

optimizing the operation of reservoir systems. *Journal of Water Resources Planning and Management* **141** (8), 04014097.

Buchtele, J. 1993 Runoff changes simulated using a rainfall-runoff model. *Water Resources Management* **7** (4), 273–287.

Burn, D. H. & Simonovic, S. P. 1996 Sensitivity of reservoir operation performance to climatic change. *Water Resources Management* **10** (6), 463–478.

Fallah-Mehdipour, E., Haddad, O. B. & Mariño, M. A. 2011 MOPSO algorithm and its application in multipurpose multireservoir operations. *Journal of Hydroinformatics* **13** (4), 794–811.

Fallah-Mehdipour, E., Haddad, O. B. & Mariño, M. A. 2013 Developing reservoir operational decision rule by genetic programming. *Journal of Hydroinformatics* **15** (1), 103–119.

Gohari, A., Mirchi, A. & Madani, K. 2017 Erratum to: system dynamics evaluation of climate change adaptation strategies for water resources management in central Iran. *Water Resources Management* **31**, 4367–4368.

Hassan, Z., Shamsudin, S. & Harun, S. 2014 Application of SDSM and LARS-WG for simulating and downscaling of rainfall and temperature. *Theoretical and Applied Climatology* **116** (1–2), 243–257.

Intergovernmental Panel on Climate Change (IPCC) 1999 *Summary for Policymakers and Technical Summary of the Working Group I Report (1995)*. Cambridge University Press, Cambridge, UK.

Intergovernmental Panel on Climate Change (IPCC) 2014 Climate change 2007: The physical science basis. In: *Contribution of Working Group I to the Fourth Assessment rep. of the Intergovernmental Panel on Climate Change* (S. Solomon, D. Qin, M. Manning, Z. Chen, M. Marquis, K. Averyt, M. Tingor & H. L. Miller, eds). Cambridge University Press, Cambridge, UK.

Jakeman, A. J. & Hornberger, G. M. 1993 How much complexity is warranted in a rainfall-runoff model? *Water Resources Research* **29** (8), 2637–2649.

Kamperman, H. & Biesbroek, R. 2017 Measuring progress on climate change adaptation policy by Dutch water boards. *Water Resources Management* **31** (14), 4557–4570.

Katz, R. W. 2002 Techniques for estimating uncertainty in climate change scenarios and impact studies. *Climate Research* **20** (2), 167–185.

Kisi, O. 2011 Wavelet regression model as an alternative to neural networks for river stage forecasting. *Water Resources Management* **25** (2), 579–600.

Nezhad, S. M., Mashal, M. & Hedayat, N. 2013 Simulation of the climate change impact on runoff in the Dez dam area. *International Journal of Agriculture and Crop Sciences* **6** (3), 121–126.

Niknam, T., Sharifinia, S. & Azizipanah-Abarghooee, R. 2013 A new enhanced bat-inspired algorithm for finding linear supply function equilibrium of GENCOs in the competitive electricity market. *Energy Conversion and Management* **76**, 1015–1028.

Ostadrahimi, L., Mariño, M. A. & Afshar, A. 2012 Multi-reservoir operation rules: multi-swarm PSO-based optimization approach. *Water Resources Management* **26** (2), 407–427.

Santos, C., Monteiro, A. T., Azevedo, J. C., Honrado, J. P. & Nunes, J. P. 2017 Climate change impacts on water resources and reservoir management: uncertainty and adaptation for a mountain catchment in northeast Portugal. *Water Resources Management* **31** (11), 3355–3370.

Wang, J. F., Cheng, G. D., Gao, Y. G., Long, A. H., Xu, Z. M., Li, X. & Barker, T. 2008 Optimal water resource allocation in arid and semi-arid areas. *Water Resources Management* **22** (2), 239–258.

Wang, K. W., Chang, L. C. & Chang, F. J. 2011 Multi-tier interactive genetic algorithms for the optimization of long-term reservoir operation. *Advances in Water Resources* **34** (10), 1343–1351.

Xu, C. Y. 1999 Climate change and hydrologic models: a review of existing gaps and recent research developments. *Water Resources Management* **13** (5), 369–382.

Xu, C. Y. 2000 Review on regional water resources assessment models under stationary and changing climate. *Water Resources Management* **18** (6), 591–612.

Yang, X. S. & Hossein Gandomi, A. 2012 Bat algorithm: a novel approach for global engineering optimization. *Engineering Computations* **29** (5), 464–483.

Yang, G., Guo, S., Liu, P., Li, L. & Liu, Z. 2017a Multiobjective cascade reservoir operation rules and uncertainty analysis based on PA-DDS algorithm. *Journal of Water Resources Planning and Management* **143** (7), 04017025.

Yang, T., Asanjan, A. A., Welles, E., Gao, X., Sorooshian, S. & Liu, X. 2017b Developing reservoir monthly inflow forecasts using artificial intelligence and climate phenomenon information. *Water Resources Research* **53** (4), 2786–2812.

Zavadskas, E. K., Turskis, Z., Antucheviciene, J. & Zakarevicius, A. 2012 Optimization of weighted aggregated sum product assessment. *Elektronika ir Elektrotechnika* **122** (6), 3–6.

Zhang, W., Liu, P., Wang, H., Lei, X. & Feng, M. 2017 Operating rules of irrigation reservoir under climate change and its application for the Dongwushi Reservoir in China. *Journal of Hydro-Environment Research* **16**, 34–44.

First received 19 July 2017; accepted in revised form 13 January 2018. Available online 8 February 2018